PHYSICAL REVIEW D **82,** 083524 (2010)

# Proliferation of sharp kinks on cosmic (super)string loops with junctions

P. Binétruy,* A. Bohé,† T. Hertog,‡ and D. A. Steer§

*APC, 10 rue Alice Domon et Léonie Duquet, 75205 Paris Cedex 13, France and Université Paris-Diderot, CNRS/IN2P3, CEA/IRFU and Observatoire de Paris, France*

(Received 13 July 2010; published 26 October 2010)

Motivated by their effect on the gravitational wave signal emitted by cosmic strings, we study the dynamics of kinks on strings of different tensions meeting at junctions. The propagation of a kink through a $Y$ junction leads to the formation of three ''daughter'' kinks. Assuming a uniform distribution of the incoming wave vectors at the junction, we find there is a significant region of configuration space in which the sharpness of at least one of the daughter kinks is enhanced relative to the sharpness of the initial kink. For closed loops with junctions we show this leads to an exponential growth in time of very sharp kinks. Using numerical simulations of realistic, evolving cosmic string loops with junctions to calculate the distribution of kink amplitudes as a function of time, we show that loops of this kind typically develop several orders of magnitude of very sharp kinks before the two junctions collide. This collision, or other effects such as gravitational backreaction, may end the proliferation.

DOI: 10.1103/PhysRevD.82.083524 PACS numbers: 98.80.Cq, 11.27.+d

## I. INTRODUCTION

In recent years there has been a revival in the study of cosmic strings and cosmic superstrings, motivated largely by the realization that cosmic superstrings can form as a by-product of brane inflation (see, e.g., [1–5] for reviews). Of crucial importance is the fact that their observational signatures may provide a unique window on string theory. Hence much work has been dedicated to studying the evolution of cosmic superstring networks (see, e.g., [6–11]) and to determining, e.g., their gravitational wave signatures [12–15], which may be detectable by future experiments such as LISA.

The properties of cosmic superstrings differ in at least three ways from those of standard cosmic strings, whose evolution and observational signatures have been studied in depth for over 30 years. First, a network of cosmic superstrings contains different types of strings, each with a different tension: fundamental $F$ strings; D1-branes or $D$ strings; and $(p, q)$ strings which are a bound state of $p$ $F$ strings and $q$ $D$ strings. Second, a network of cosmic superstrings is thought to contain numerous $Y$ junctions, namely, points at which $F$ and $D$ strings meet to form the bound state $(p, q)$ string. Finally, whereas the intercommutation probability for standard cosmic strings is $P = 1$, this is much reduced for cosmic superstrings [16]. Indeed, for the collision of two $F$ strings, $10^{-3} \lesssim P_F \lesssim 1$, whereas for the collision of two $D$ strings, $0.1 \lesssim P_D \lesssim 1$. When strings of different types (such as an $F$ string and a $D$ string) collide, they cannot intercommute due to flux conservation. In certain cases [17,18] they form a bound state string with two corresponding $Y$ junctions.

Earlier studies on the detectability of standard cosmic strings through their gravitational wave emission have recently been partly generalized to cosmic superstrings [12–14]. In these papers cosmic superstrings were modeled as usual cosmic strings, but with a reduced intercommutation probability $P \leq 1$. However, until now, the effects of junctions and bound states, as well as the implications of having strings with different tensions, have not been taken into account.

In this and in a companion paper [19], we study the effect of junctions on the gravitational wave burst emission from cosmic string networks [20]. It is well-known that gravitational radiation from cosmic string loops is dominated by the lowest frequency modes (which are a multiple of the fundamental frequency for loops without junctions) [21]. Superimposed on the stochastic background of gravitational waves they generate are high frequency bursts emitted at cusps and kinks [22]. Kinks, in particular, radiate as they propagate along a string and through a junction, and when they interact with other kinks [23]. Cusps on the other hand are punctual in time, but generate bursts with a higher amplitude.

For cosmic strings without junctions, cusps provide the dominant contribution to the gravitational wave (GW) burst signal. In [24] cusps have been argued to be a generic feature on strings with junctions as well. More recently, however, it has been shown [25] that since cosmic superstrings evolve in a higher dimensional space-time, cusps may be very rare events and furthermore those cusps which are formed are rounded off, hereby significantly reducing their GW burst signal.

For this and other reasons we focus on kinks in this paper. On a loop with no junctions, the number of kinks is constant, fixed by the initial configuration of that loop. However, for a loop containing junctions this is no longer the case. Such loops evolve nonperiodically in time, and as we will see, the number of kinks on them increases rapidly:

*binetruy@apc.univ-paris7.fr
†bohe@apc.univ-paris7.fr
‡hertog@apc.univ-paris7.fr
§steer@apc.univ-paris7.fr

 

kinks proliferate. Here we calculate how the number of large amplitude (that is, very sharp) kinks proliferates as the loop evolves, since these will turn out to dominate the GW signal from kinks on loops with junctions [19].

The paper is organized as follows. In Secs. II and III, we focus on the interaction between a kink and a single junction. (That is, we do not as yet consider closed loops—this is done in Secs IV and V.) In Sec. II we use the dynamical equations of motion for strings with junctions derived in [17] to show that when a kink propagates through a $Y$ junction, it leads to the formation of three ''daughter'' kinks (one reflected, and two transmitted). For a specific junction configuration for which the whole evolution can be solved analytically, we show explicitly that the amplitude of the daughter kinks may be larger than that of the original ''parent'' kink [26]. In Sec. III we generalize this discussion by considering arbitrary junction configurations. More specifically, we take a uniform distribution of incoming waves at the junction and of incoming kink amplitudes and show that, in a significant region of configuration space, the amplitude of at least one of the daughter kinks is larger than that of the parent kink.

In Secs. IV and V we study the evolution of the number of sharp kinks on closed loops with junctions. In Sec. IV, we consider a simplified model of a loop with junctions that does not take into account the complicated dynamics of the loop itself, and we argue that the number of large amplitude kinks increases exponentially with time. Finally, the dynamics of the loop is taken into account in Sec. V, where we show that this dynamics generally further enhances the proliferation of sharp kinks. Our conclusions are presented in Sec. VI.

## II. PROPAGATION OF A KINK THROUGH A JUNCTION

In this section, following [17], we first review the equations of motion for three semi-infinite Nambu-Goto strings of tensions $\mu_1$, $\mu_2$ and $\mu_3$ which meet at a $Y$ junction. A consequence of these equations is that the propagation of a kink through a $Y$ junction results in the production of three daughter kinks: a reflected kink as well as two transmitted kinks. We also define kink amplitude (or sharpness), and analytically study—in the simplest case of an initially static junction—the amplitude of the daughter kinks, showing that in some cases these can be amplified relative to the incoming kink.

### A. Description of the system

We work in flat space-time with signature $(-+++)$, and use the standard conformal-temporal gauge so that each string is described by its spatial coordinates $\mathbf{x}_j(\sigma, t)$, where $t$ coincides with Lorentz time and the subscript $j$ labels the different strings. The gauge constraints can then be written as (with $'$ and $\dot{}$ standing for derivatives with respect to $\sigma$ and $t$, respectively)

$$\mathbf{x}_j' \cdot \dot{\mathbf{x}}_j = 0, \tag{1}$$

$$\mathbf{x}_j'^2 + \dot{\mathbf{x}}_j^2 = 1. \tag{2}$$

The action describing the combined system of three semi-infinite strings meeting at a junction has been analyzed in [17]. Away from the junction the wavelike equation of motion for each string has solution

$$\mathbf{x}_j(\sigma, t) = \frac{1}{2}(\mathbf{a}_j(u) + \mathbf{b}_j(v)), \tag{3}$$

where

$$u = \sigma + t, \qquad v = \sigma - t, \tag{4}$$

and where $\mathbf{a}_j'^2 = \mathbf{b}_j'^2 = 1$ in order to satisfy the gauge constraints. Each string is bounded by the junction located at $\mathbf{X}(t) = \mathbf{x}_i(s_i(t), t)$. One can therefore let $\sigma$ take values in the interval $]-\infty, s_j(t)]$.

As explained in [17], the initial conditions for $\dot{\mathbf{x}}_j$ and $\mathbf{x}_j'$ at $t = 0$ determine $\mathbf{a}_j(u)$ and $\mathbf{b}_j(v)$ for $u \leq s_j(0)$ and $v \leq s_j(0)$. A set of coupled differential equations describing the physics at the junction then enables one to determine the evolution of $s_j(t)$ as well as the outgoing waves $\mathbf{a}_j'(s_j(t) + t)$ in terms of the incoming waves $\mathbf{b}_j'(s_j(t) - t)$ (which are determined by the initial conditions since $\dot{s}_j \leq 1$). In particular, let

$$\nu_1 = \mu_2 + \mu_3 - \mu_1 \geq 0, \tag{5}$$

$$\begin{aligned} M_1 &= \mu_1^2 - (\mu_2 - \mu_3)^2 = \nu_2\nu_3 \geq 0, \\ c_1(t) &= \mathbf{b}_2'(s_2(t) - t) \cdot \mathbf{b}_3'(s_3(t) - t), \end{aligned} \tag{6}$$

and circular permutations, as well as

$$\mu = \mu_1 + \mu_2 + \mu_3. \tag{7}$$

Then the equations of motion imply energy conservation at the junction

$$\mu_1\dot{s}_1 + \mu_2\dot{s}_2 + \mu_3\dot{s}_3 = 0. \tag{8}$$

One also has

$$\frac{\mu_j(1 - \dot{s}_j)}{\mu} = \frac{M_j(1 - c_j)}{M_1(1 - c_1) + M_2(1 - c_2) + M_3(1 - c_3)} \tag{9}$$

and

$$\mathbf{a}_j'(s_j(t) + t) = \frac{1}{1 + \dot{s}_j}\Big[(1 - \dot{s}_j)\mathbf{b}_j'(s_j(t) - t) - \frac{2}{\mu}\sum_{k=1}^{3}\mu_k(1 - \dot{s}_k)\mathbf{b}_k'(s_k(t) - t)\Big] \tag{10}$$

which determines the outgoing wave on string $j$ in terms of the inward moving waves. The last term in (10) is proportional to the velocity of the junction:

$$\dot{\mathbf{X}} = -\frac{1}{\mu}\sum_{k=1}^{3}\mu_k(1-\dot{s}_k)\mathbf{b}'_k(s_k(t)-t). \tag{11}$$

From (10) it follows that if one of the strings has a kink propagating towards the junction, i.e., one of the functions $\mathbf{b}'_j(v)$ has a discontinuity, then all $\mathbf{a}'_j(u)$ acquire a discontinuity when the kink reaches the junction. The presence of the junction therefore increases the number of kinks in the system from 1 to 3. We refer to the three newly formed kinks as "daughter kinks."

Furthermore, Eq. (10) also implies that for essentially all initial conditions fixed at $t = 0$, say, the subsequent evolution always generates kinks. Indeed, from Eq. (10) and for $t = 0^+$, $\mathbf{a}'_j(s_j(0)^+)$ on string $j$ is determined by the weighted sum of all $\mathbf{b}'_k(s_k(0)^-)$. The latter are fixed by the arbitrary initial conditions and independent of the $\mathbf{a}'_k(s_k(0)^-)$. Their sum therefore yields a vector $\mathbf{a}'_j(s_j(0)^+)$ which is generally different from $\mathbf{a}'_j(s_j(0)^-)$. Therefore $\mathbf{a}'_j$ will be discontinuous [27] at $u = s_j(0)$, leading to a kink $t = 0^+$. Hence the presence of junctions essentially implies the existence of kinks, which therefore will not need to be introduced by hand in our simulations below.

### B. Amplitude and transmission coefficients

Kinks on cosmic strings are sources of gravitational wave bursts: a kink emits bursts throughout its propagation on the string [22], and also when it encounters another kink or when it crosses a junction [23]. However, the GW signal emanating from kinks on a network of strings is determined not only by their number, but also by their amplitudes. The kink amplitude can be defined as follows.

Consider a kink moving towards a junction [i.e., a discontinuity of $\mathbf{b}'_j(v)$ at $v_*$]. The amplitude of all GW bursts associated with kinks is proportional to the components of [22,23]

$$\left(\frac{\mathbf{b}'_j(v_*^+)}{1-\mathbf{n}\cdot\mathbf{b}'_j(v_*^+)} - \frac{\mathbf{b}'_j(v_*^-)}{1-\mathbf{n}\cdot\mathbf{b}'_j(v_*^-)}\right). \tag{12}$$

Both denominators in (12) are generically comparable and of order 1, because the direction of emission $\mathbf{n}$ is *a priori* uncorrelated with $\mathbf{b}'_j(v_*^+)$ and $\mathbf{b}'_j(v_*^-)$, and therefore (12) is of order $\|\mathbf{b}'_j(v_*^+) - \mathbf{b}'_j(v_*^-)\|$. We define the kink amplitude or sharpness by

$$A[\mathbf{b}'_j] = \frac{1}{2}\|\mathbf{b}'_j(v_*^+) - \mathbf{b}'_j(v_*^-)\| = |\sin(\theta/2)|, \tag{13}$$

where $\theta$ is the angle between $\mathbf{b}'_j(v_*^\pm)$. The factor of $1/2$ is a normalization factor so that $0 \le A[\mathbf{b}'_j] \le 1$. We adopt an analogous definition of the sharpness of an outward moving kink on string $j$ characterized by a discontinuity in $\mathbf{a}'_j(u)$.

At first sight one might expect the daughter kinks to have smaller amplitudes than the incoming kink. However, this is not the case. In particular energy conservation at the junction, Eq. (8), does not constrain the amplitude of the transmitted kinks [29]. Indeed the derivatives in (8) suffer a discontinuity when a kink hits the junction, and these therefore undergo a sudden jump.

It will also be useful to define the following transmission coefficients $C_j$. For instance, consider a kink that propagates towards the junction on string 1 [i.e., $\mathbf{b}'_1(v)$ has a discontinuity at $v_{1*}$] and reaches the junction at $t_*$, with $v_{1*} = s_1(t_*) - t_*$. Then each function $\mathbf{a}'_j(u)$ acquires a discontinuity at $u_{j*} = s_j(t_*) + t_*$. We define

$$C_j = \frac{A[\mathbf{a}'_j]}{A[\mathbf{b}'_1]}, \tag{14}$$

where the amplitudes are given by Eq. (13).

### C. Example: Static junction

To conclude this section, we illustrate the production of daughter kinks with an example that can be worked out analytically.

The strings of tension $\mu_1$ and $\mu_2 = \mu_3$ are taken to be in the $(x, y)$ plane at all times, and the initial configuration considered is shown in the left-hand panel of Fig. 1. String 1 lies along the $x$ axis, and strings 2 and 3 subtend an angle $\psi$ with respect to the $y$ axis, chosen such that the junction is initially static. There are two kinks on string 1, both of which propagate towards the junction (they are discontinuities in $\mathbf{b}'_1$). Once both kinks have propagated through the junction, the angles between the strings at the junction are again the same as initially and hence the junction is again static. However, all three strings now have outward moving kinks on them as shown in the right-hand panel of Fig. 1. The amplitude of the outgoing kinks can be calculated as follows.

Let

$$\begin{aligned} \mathbf{k}_1 &= (-1, 0), \qquad & \mathbf{k}_1^\theta &= -(\cos\theta, \sin\theta), \\ \mathbf{k}_2 &= (\epsilon, -\delta), \qquad & \mathbf{k}_3 &= (\epsilon, \delta), \end{aligned} \tag{15}$$

where $\theta \in [-\pi, \pi]$ is a free parameter and we have defined

$$0 \le \epsilon \equiv \frac{\mu_1}{2\mu_2} \le 1, \qquad \delta \equiv \sqrt{1-\epsilon^2}. \tag{16}$$

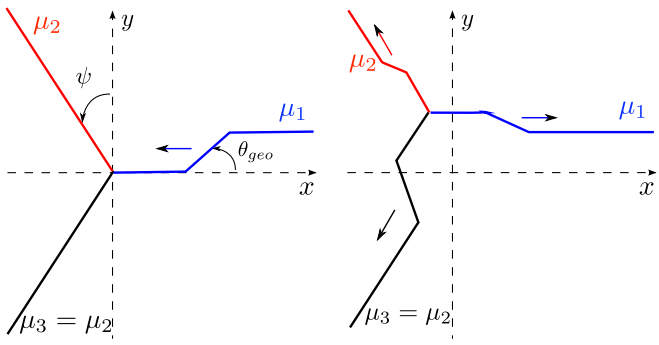


FIG. 1 (color online). Propagation of two kinks through an initially static junction. Initial (left) and final (right) configuration of the system.

Hence the angle $\psi = \arctan(\epsilon/\delta)$. Then the initial condition corresponding to Fig. 1 is given by

$$\mathbf{a}_1'(u) = \mathbf{k}_1,$$
$$\mathbf{a}_2'(u) = \mathbf{k}_2, \quad \text{and} \quad \mathbf{a}_3'(u) = \mathbf{k}_3 \quad \text{if } u \le 0,$$
$$\mathbf{b}_1'(v) = \begin{cases} \mathbf{k}_1 & \text{if } -L \le v \le 0 \\ \mathbf{k}_1^\theta & \text{if } -L-\ell \le v \le -L \\ \mathbf{k}_1 & \text{if } v \le -L-\ell, \end{cases}$$
$$\mathbf{b}_2'(v) = \mathbf{k}_2 \quad \text{and} \quad \mathbf{b}_3'(v) = \mathbf{k}_3 \quad \text{if } v \le 0.$$

From (3) it now follows that for string 1 and for $v \in [-L-\ell, -L]$,

$$\begin{aligned} \mathbf{x}_1' &= \cos(\theta/2)(\cos(\theta/2), \sin(\theta/2)), \\ \dot{\mathbf{x}}_1 &= \sin(\theta/2)(\sin(\theta/2), -\cos(\theta/2)). \end{aligned} \tag{17}$$

Thus the physical angle to the $x$ axis made by the segment of string 1 between the two kinks is $\theta_{\text{geo}} = \theta/2$. It moves with velocity $\sin(\theta/2)$ towards the junction.

From the equations of motion (6)–(10) one can analytically determine the evolution of the system, since the $\mathbf{b}_j'$ are piecewise constant functions. The evolution consists of three distinct phases:

(i) $t \in [0, L]$:
The solutions of $c_j$ in (6), substituted into (9), yield $\dot{s}_j = 0$ on each string. Thus (11) implies the junction is indeed static: $\dot{\mathbf{X}} = 0$ [17]. The outgoing waves are determined by (10): $\mathbf{a}_j'(u) = \mathbf{k}_j$ for $u \in [0, L]$. Hence during this phase, the segment between the two kinks propagates towards the junction with velocity $|\sin(\theta/2)|$ while the rest of the system remains static. This phase ends when $t = L$, because then $s_1(t = L) - L = v = -L$ so the scalar products $c_j(t)$ [which depend on $\mathbf{b}_1'(s_1(t) - t)$] change.

(ii) $t \in [L, t_*]$:
During this phase the segment between the two kinks crosses the junction and $\mathbf{b}_1' = \mathbf{k}_1^\theta$. The time $t_*$ is the solution to $s_1(t_*) - t_* = -L - \ell$. Beyond this time, $\mathbf{b}_1'$ changes back to $\mathbf{k}_1$ again. From (9) we find that the $\dot{s}_j$ are constant and equal to

$$\dot{s}_1 = \frac{\epsilon(\cos\theta - 1)}{\epsilon\cos\theta + (1 + \epsilon + \epsilon^2)}, \tag{18}$$

$$\dot{s}_2 = \frac{(1 - \cos\theta)\epsilon^2 - \delta\sin\theta(1 + \epsilon)}{\epsilon\cos\theta + (1 + \epsilon + \epsilon^2)}, \tag{19}$$

$$\dot{s}_3 = \frac{(1 - \cos\theta)\epsilon^2 + \delta\sin\theta(1 + \epsilon)}{\epsilon\cos\theta + (1 + \epsilon + \epsilon^2)} = -(\dot{s}_1 + \dot{s}_2). \tag{20}$$

Thus $s_j(t) = \dot{s}_j(t - L)$, so that $t_* = L + \frac{\ell}{1-\dot{s}_1}$. The functions $\mathbf{a}_j'$ can then be obtained from (10); for instance,

$$\mathbf{a}_1'(u) = \frac{1}{1 + \epsilon^2 + 2\epsilon\cos\theta}(-(1 + \epsilon^2)\cos\theta - 2\epsilon, \delta^2\sin\theta), \tag{21}$$
$$u \in \left[L, L + \frac{1 + \dot{s}_1}{1 - \dot{s}_1}\right].$$

Finally Eq. (11) determines the constant velocity of the junction during this time interval:

$$\dot{\mathbf{X}} = \frac{1}{1 + \epsilon + \epsilon^2 + \epsilon\cos\theta}(\epsilon(\cos\theta - 1), (1 + \epsilon\sin\theta)). \tag{22}$$

(iii) $t > t_*$:
The configuration at the junction is now exactly the same as during the first phase. That is, $\dot{s}_j = 0$ on each string and $\mathbf{a}_j'(u) = \mathbf{k}_j$ for $u > L + \frac{1+\dot{s}_j}{1-\dot{s}_1}$. Now, however, there is a segment between two kinks on each string and it propagates away from the junction as depicted in the right panel of Fig. 1.

Calculation of the transmission coefficients (14) when the first kink encounters the junction yields

$$C_1(\theta, \epsilon) = \frac{(1 - \epsilon)}{\sqrt{2\epsilon\cos\theta + \epsilon^2 + 1}} \le 1, \tag{23}$$

$$C_2(\theta, \epsilon) = \frac{2\epsilon}{\sqrt{(1 + \epsilon + 2\epsilon^2) + \epsilon(1 - \epsilon)\cos\theta - (1 + \epsilon)\sqrt{1 - \epsilon^2}\sin\theta}}, \tag{24}$$

$$C_3(\theta, \epsilon) = C_2(-\theta, \epsilon). \tag{25}$$

In Fig. 2 we plot the transmission coefficients [30] for different values of the string tensions in the allowed range $0 \le \epsilon = \mu_1/2\mu_2 \le 1$. One sees that, in this particular example, the reflected kink on string 1 always has a smaller amplitude than the incoming kink, though the reduction in amplitude is generally rather weak for incoming kinks on the lightest string.

By contrast, the transmitted kinks can be amplified. When all tensions are equal ($\epsilon = 1/2$), this occurs for a rather broad set of (static) junction configurations. However, for $\epsilon \to 0$ (that is, when strings 2 and 3 are heavy compared to string 1), we find $C_2 > 1$ only in a limited range of $\theta$. In this regime, it is in fact straightforward to understand the position of the peak. From (10) it follows that the amplitude $A[\mathbf{a}_j']$—and hence the transmission coefficient $C_j$—is large when after the kink has crossed the junction, the corresponding $\dot{s}_j \to -1$. Equation (19) predicts that, for small $\epsilon$, this occurs on string 2 when $\sin\theta = 1$ or $\theta = \pi/2$, as is indeed

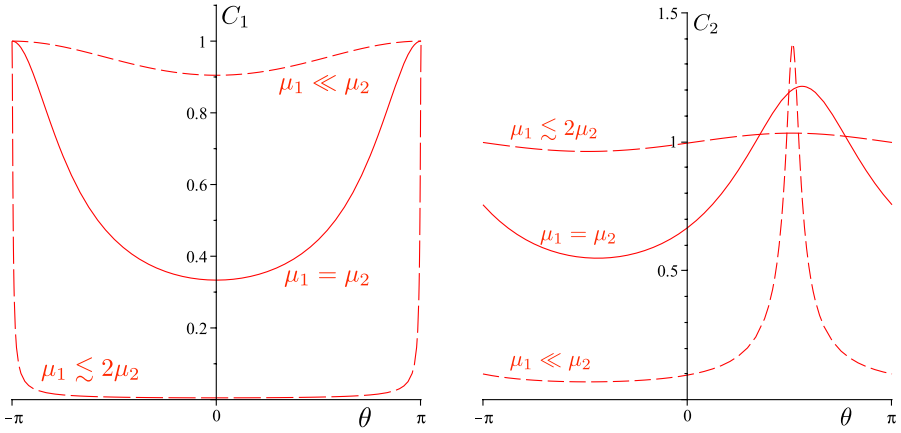


FIG. 2 (color online). Transmission coefficients $C_1$ and $C_2$ as functions of $\theta$ for three different ratios of tensions $\mu_1$ and $\mu_2$. The tension $\mu_3$ of the third string is taken to be equal to $\mu_2$ in all three cases.

the case in Fig. 2. Away from its sharp peak, $C_2 \sim \epsilon$ for small $\epsilon$, as can be seen from Eq. (24). Finally, for $\epsilon \sim 1$, $C_2$ is always close to 1 even though slight amplification can occur in a broad range of $\theta$.

We should stress that the above discussion is limited to the specific junction configuration of Fig. 1. We now turn to arbitrary junction configurations.

## III. DISTRIBUTIONS OF TRANSMISSION COEFFICIENTS

In this section we aim to gain intuition on the distributions of transmission coefficients characterizing the propagation of kinks through junctions in a more generic context. Namely, we study the statistical properties of the $C_j$ using an underlying uniform distribution of junction configurations. We would like to answer the following question: is amplification frequent or not?

To specify the configuration of the junction just before the arrival of the incoming kink as well as the amplitude of the kink, one needs four incoming unit vectors. We consider a kink moving towards the junction on string 1, specified by a discontinuity in $\mathbf{b}_1'(v)$ at $v_{1*}$. Let $t_*$ be the time when the kink reaches the junction. Then the amplitudes of the transmitted kinks depend on $\mathbf{b}_1'(v_{1*}^+)$, $\mathbf{b}_1'(v_{1*}^-)$, $\mathbf{b}_2'(s_2(t_*) - t_*)$ and $\mathbf{b}_3'(s_3(t_*) - t_*)$, for which we will use the more concise notation $\mathbf{b}_1'^+$, $\mathbf{b}_1'^-$, $\mathbf{b}_2'$ and $\mathbf{b}_3'$. Equation (10) then yields

$$\mathbf{a}_1'^{\pm} = P_1^{\pm}\mathbf{b}_1'^{\pm} - Q_{1,2}^{\pm}\mathbf{b}_2' - Q_{1,3}^{\pm}\mathbf{b}_3', \tag{26}$$

$$\mathbf{a}_2'^{\pm} = P_2^{\pm}\mathbf{b}_2' - Q_{2,3}^{\pm}\mathbf{b}_3' - Q_{2,1}^{\pm}\mathbf{b}_1'^{\pm}, \tag{27}$$

$$\mathbf{a}_3'^{\pm} = P_3^{\pm}\mathbf{b}_3' - Q_{3,1}^{\pm}\mathbf{b}_1'^{\pm} - Q_{3,2}^{\pm}\mathbf{b}_2', \tag{28}$$

where

$$P_i^{\pm} = \left(\frac{1 - \dot{s}_i^{\pm}}{1 + \dot{s}_i^{\pm}}\right)\left(\frac{\nu_i}{\mu}\right), \qquad Q_{i,j}^{\pm} = \left(\frac{2\mu_j}{\mu}\right)\left(\frac{1 - \dot{s}_j^{\pm}}{1 + \dot{s}_i^{\pm}}\right) \tag{29}$$

and the $\dot{s}_j^{\pm}$ are given by Eq. (9). Using Eqs. (26)–(28), the transmission coefficients $C_j$ can be obtained from (14). Our aim here is to determine their probability distributions. Here we focus on the case of equal tensions. Unequal tensions are studied in Appendix A.

The configuration of the junction just before the arrival of the kink is specified by the unit vectors $\mathbf{b}_1'^-$, $\mathbf{b}_2'$ and $\mathbf{b}_3'$. We assume for now that these are independent, with uniform distributions on the unit sphere. We also assume a flat distribution in the incoming kink, namely, a uniform distribution on the unit sphere for $\mathbf{b}_1'^+$ (and, in particular, independence of $\mathbf{b}_1'^+$ of the other unit vectors) [31].

Given these assumptions, we numerically calculate the distributions of the transmission coefficient by drawing a large number (typically $N = 3 \times 10^7$) of random configurations at the junction in order to estimate the various statistical quantities of interest.

### A. Marginal distributions $p(C_j)$

We are in the first place interested in the joint distribution $p(C_1, C_2, C_3)$ from which one could determine, for example, the probability for several kinks to be amplified at the same time. However, as a warm-up, we show in Fig. 3 the marginal distributions $p(C_j)$, for the case of equal tensions $\mu_j = 1$. These distributions $p(C_j)$ have a large tail where $C_j > 1$, indicating that both the reflected and the transmitted kinks can be amplified in a significant part of configuration space. Indeed, $P(C_1 > 1) = 0.11$, $P(C_2 > 1) = 0.19 = P(C_3 > 1)$.

However, as expected from the static example of Sec. II C, the marginal distributions depend significantly on the ratios of string tensions. In Appendix A we discuss the distributions for various other sets of tensions, including several limiting cases where, using the smallness of some of the coefficients (29), analytic arguments can explain certain features of the distributions.

### B. Simultaneous amplification of transmission coefficients

In order to understand how the total number of large amplitude kinks on strings containing $Y$ junctions changes in time, one really needs the joint distribution $p(C_1, C_2, C_3)$ which contains information about the correlations between the different transmission coefficients.

The simplest question to ask involving correlations between the $C_j$ is the following: when a kink reaches a junction, what is the probability that at least one of the three daughter kinks is amplified (so at least one of the $C_j > 1$)? This probability may well be significantly larger than that suggested by the tails of the individual daughter kink distributions discussed above. In the case of equal tensions $\mu_i = 1$ corresponding to Fig. 3 we find

$$P(\text{at least one amplification}) = 0.43 \quad \text{for } \mu_j = 1. \quad (30)$$

Amplification is therefore not such a rare event, and hence we have a first hint that the number of large amplitude kinks may grow significantly in a system in which the total number of kinks increases due to the presence of $Y$ junctions.

In a similar way, the probability of having at least two simultaneous amplifications is

$$P(\text{at least two amplifications}) = 0.07 \quad \text{for } \mu_j = 1. \quad (31)$$

Again those probabilities are not negligible and such events can contribute importantly to the enhancement of the number of large amplitude kinks in an interconnected network [33]. In the table below, we summarize the amplification probabilities for the different sets of tensions considered here and in Appendix A.

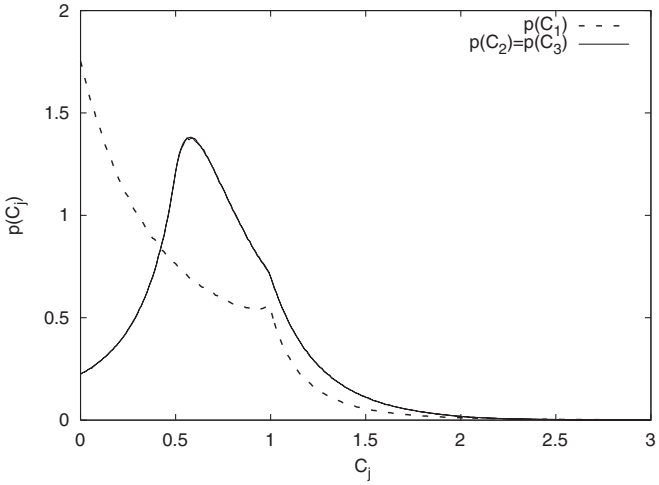


FIG. 3. Marginal distributions $p(C_j)$ of the transmission coefficients $C_j$ for equal tensions $\mu_j = 1$ and a uniform distribution of junction configurations. The average values are $\langle C_1 \rangle = 0.49$, $\langle C_2 \rangle = 0.72$, $\langle C_3 \rangle = 0.72$.

### C. Joint distribution $p(C_1, C_2, C_3)$

Even though there is a significant region of configuration space in which the amplitude of at least one of the daughter kinks is enhanced relative to the amplitude of the initial kink, it is important to know whether the amplitude of the remaining kinks is typically significantly reduced in such events. Figure 4 shows two-dimensional slices through the joint distribution $p(C_1, C_2, C_3)$ for four different values of $C_1$, again with $\mu_j = 1$. (Note that the grey scale differs from one panel to the next.) The horizontal and vertical axes label $C_2$ and $C_3$ respectively.

The joint probability distribution exhibits the following important features:

| Tensions | $P(C_1 > 1)$ | $P(C_2 > 1)$ | $P(C_3 > 1)$ | $P$ (at least 1 amp) | $P$ (at least 2 amp) |
|---|---|---|---|---|---|
| $\mu_1 = 0.1, \mu_2 = 1, \mu_3 = 1$ | 0.12 | 0.01 | 0.01 | 0.12 | 0.004 |
| $\mu_1 = 1, \mu_2 = 0.1, \mu_3 = 1$ | 0.01 | 0.19 | 0.19 | 0.65 | 0.006 |
| $\mu_1 = 1.9, \mu_2 = 1, \mu_3 = 1$ | 0.12 | 0.47 | 0.47 | 0.93 | 0.11 |
| $\mu_1 = 1, \mu_2 = 1.9, \mu_3 = 1$ | 0.01 | 0.49 | 0.01 | 0.19 | 0.004 |
| $\mu_1 = 1, \mu_2 = 1, \mu_3 = 1$ | 0.12 | 0.19 | 0.19 | 0.43 | 0.07 |
| $\mu_1 = 1, \mu_2 = 1.2, \mu_3 = 1.4$ | 0.10 | 0.11 | 0.15 | 0.31 | 0.65 |

(i) The top left-hand panel of Fig 4 shows that there is a sharp peak where all transmission coefficients take small values, $C_j \ll 1$.

(ii) The remaining three panels are for values of $C_1 \geq 0.2$. They have a clear concentration of events on a arc-shaped line, as well as events off that line at values of $C_2 \sim C_3$. These latter events saturate around $C_2 \sim C_3 \lesssim 1$ for $C_1 > 1$.

(iii) The arc-shaped lines finish on two ''amplification tails'' corresponding to values of $C_2$ or $C_3$ larger than 1. There are no events for which $C_2 \geq 1$ and $C_3 \geq 1$ simultaneously.

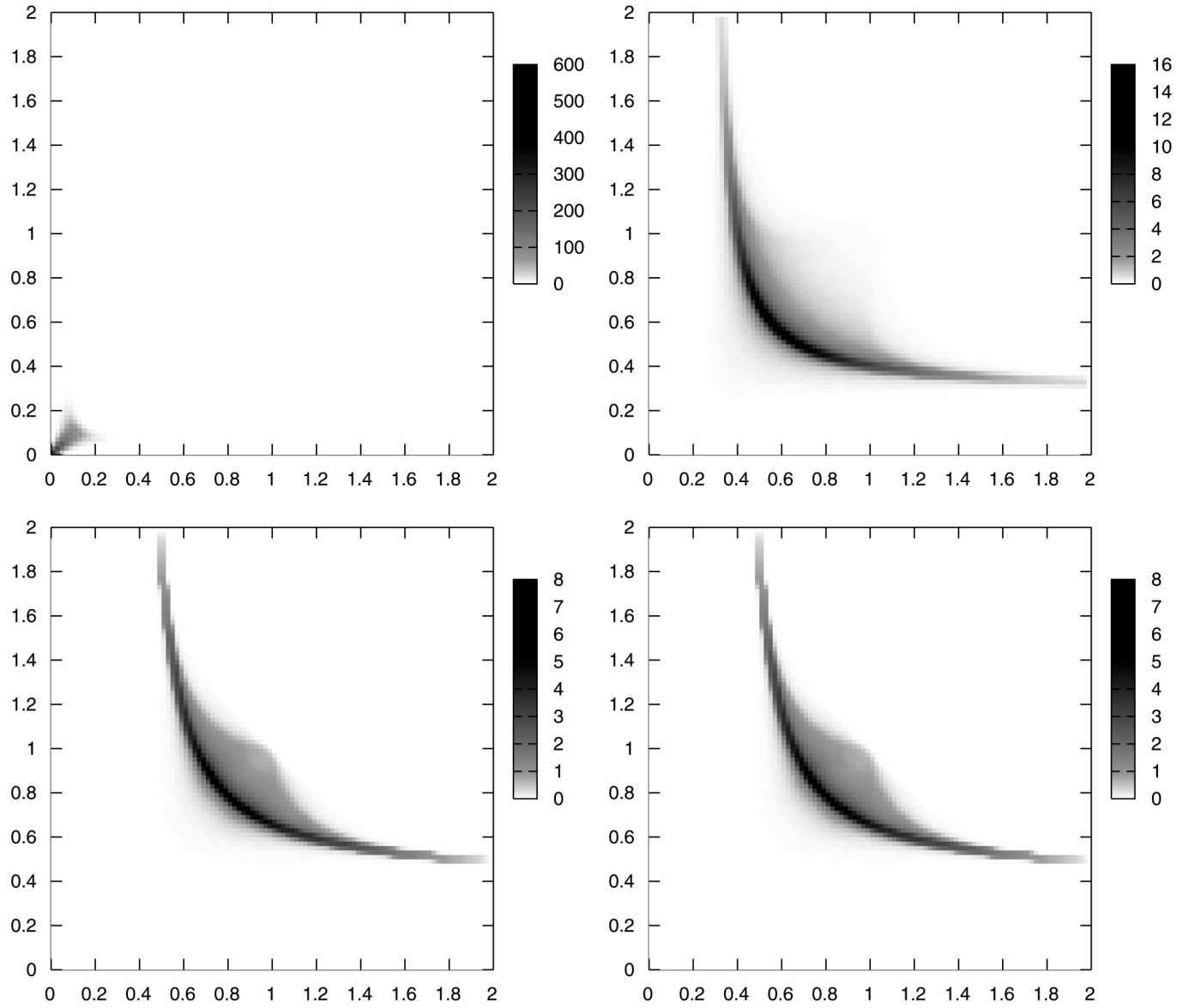

FIG. 4. Slices of the joint distribution $p(C_1, C_2, C_3)$ for four different values of $C_1$ and $\mu_j = 1$. The horizontal and vertical axes labels are $C_2$ and $C_3$, respectively. The values of $C_1$ on the different slices are $C_1 = 0$ (top left), $C_1 = 0.2$ (top right), $C_1 = 1$ (bottom left) and $C_1 = 1.5$ (bottom right). Note that the grey scale differs from slice to slice.

Based on the above properties of the joint distribution one can conclude that the bulk of the transmission events falls in one of the following categories:

(i) All daughter kinks have drastically reduced amplitudes.
(ii) All daughter kinks have slightly reduced amplitudes.
(iii) The amplitude of the reflected kink is significantly reduced, one transmitted kink is amplified and one is slightly reduced.
(iv) The reflected kink is amplified and the amplitude of the transmitted kinks is comparable to the amplitude of the incoming kink.

We note, in particular, that the amplification of one of the daughter kinks does not imply that the amplitudes of the remaining daughter kinks are small. In fact, except for the first kind of transmission—which is not considerably more frequent than the others (see Fig. 3)—the amplitude of the scattered kinks is never strongly suppressed. This indicates that amplifications, combined with the rapid growth of the total number of kinks in a system with junctions, lead to a large number of "large amplitude" kinks. The next section is devoted to a quantitative study of this phenomenon.

## IV. PROLIFERATION OF LARGE AMPLITUDE KINKS ON A LOOP WITH JUNCTIONS

We have seen that the sharpness of the daughter kinks is generally comparable and occasionally larger than that of

the incoming kink into a junction. Motivated by GW physics, it is therefore interesting to study how the number of kinks with a large amplitude (of order 1) evolves on closed loops with junctions. Indeed, a sustained growth of the number of such large amplitude kinks may well have an impact on the gravitational wave burst signal emanating from strings of this kind [19].

The total number of kinks on a closed loop with junctions increases exponentially in time: when an initial kink reaches a junction it gives rise to three daughter kinks, which in turn propagate towards another junction where they multiply again, and so forth. Even though the amplitude of most of the daughter and higher generation kinks is small, it is clear that the number of large amplitude kinks will also grow exponentially provided amplification occurs sufficiently frequently. Here we show this is indeed the case in a simple model of a loop with $Y$ junctions, based as before on an underlying uniform distribution of junction configurations at the time of arrival of the kink. The evolution of the loop, for a relatively general class of initial loop configurations, will be taken in account in Sec. V where we will see that the results obtained here remain largely valid.

### A. Setup

The simplest example of a closed system with $Y$ junctions is a loop formed by three strings meeting at two junctions, a typical example of which is shown in Fig. 5.

Our loop model is based on the following two simplifying assumptions:

(1) all three strings joining the two junctions have essentially the same constant invariant length $L$;
(2) when a kink (whose amplitude is known) reaches a junction, the configuration of the latter is randomly drawn among those that yield the correct amplitude for the original kink.

More explicitly we proceed as follows. First we specify the initial conditions at $t = 0$, namely $K$, the total number of left-moving and right-moving kinks on all three strings, as well as their amplitudes. (The initial positions of those kinks do not enter the subsequent analysis.) After an interval of time $L$, the first assumption ensures that all the initial kinks have reached a junction, but that none of their descendants have done so (recall that kinks propagate at the speed of light on the strings). Therefore, at $t = L$, the system contains $3K$ kinks, and at time $t = nL$ with $n$ an integer, the total number of kinks in the system [34] is $3^n K$. We then evaluate

$$Q_j^A(n) = \text{number of kinks on string } j \text{ of amplitude} \geq A \text{ as a function of the generation } n, \text{ or equivalently time } t = nL.$$

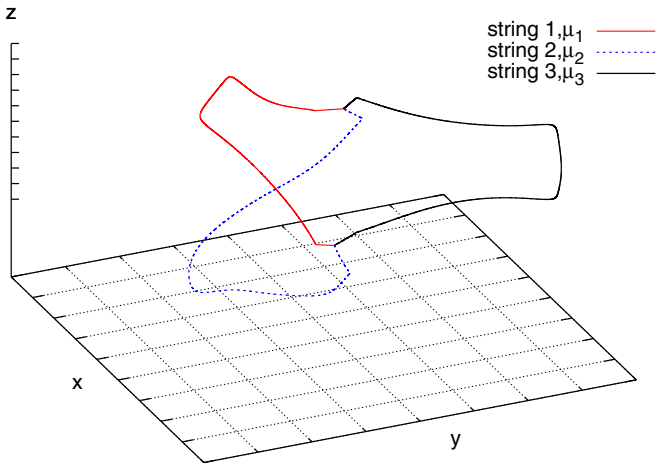


FIG. 5 (color online). A typical loop formed by 3 strings and 2 junctions.

We do so as follows. Consider a given (say, inward moving) kink of amplitude $A_i$ on string 1. Following assumption 2 we determine the amplitude of the daughter kinks by randomly drawing junction configurations, similarly to Sec. III, but now we restrict the choice to those configurations for which $\|\mathbf{b}_1'^{+} - \mathbf{b}_1'^{-}\| = A_i$. (In practice, we first draw $\mathbf{b}_1'^{-}$, $\mathbf{b}_2'$ and $\mathbf{b}_3'$ with uniform probabilities on the unit sphere and then draw $\mathbf{b}_1'^{+}$ with uniform probability on the intersection of the unit sphere and the sphere of center $\mathbf{b}_1'^{-}$ and radius $A_i$, i.e., on a circle of radius $A_i$.) In other words, instead of using the probability distribution $p(C_1, C_2, C_3)$ to draw the transmission coefficients, we use an improved version $p_{A_i}(C_1, C_2, C_3)$ that takes into account the amplitude of the incoming kink.

To summarize, for each initial kink, our model amounts to building a tree of kinks. On this tree each node represents a kink, and contains the value of its amplitude as well as the number of the string on which it arrived. It has three daughter nodes whose values are drawn randomly according to the rules explained above. At the $n$th generation, the total number of kinks is $3^n$. Clearly, as there is no interaction between kinks, for $K$ initial kinks there are $K$ trees which evolve completely independently. Hence the statistical properties of systems originally containing several kinks can be trivially deduced from those by linearity.

#### *Numerics*

Computationally, as the number of generations increases it becomes expensive to store $3^n$ amplitudes. To keep the computation manageable we divide the amplitude interval [0, 1] into $N_{\text{bin}}$ bins, and only keep track of the number of kinks on each string with an amplitude in the different bins, at each generation. To draw the amplitudes of the subsequent generation we use the center value of the bin as the amplitude of the incoming kink. That is, for kinks in bin $k > 1$, we use as an amplitude $(k - \frac{1}{2})\frac{2}{N_{\text{bin}}}$. (In our simulations, we used $N_{\text{bins}} = 100$.) Finally, we set the amplitude of kinks in the first bin to zero: we expect that after a few generations most of the kinks that lie in this bin actually have an amplitude smaller than $1/N_{\text{bin}}$ by several orders of

magnitude. Of course, this procedure can lead to an underestimation of the number of large amplitude kinks (because a few kinks from this bin must in reality be reamplified to yield large amplitude descendents) but it prevents many very small amplitude kinks from spuriously leading to large amplitude kinks. By doing this, we lose any information on the low amplitude part of the distribution (which we disregard in this paper). In our companion paper [19], we will refine this numerical setup to demonstrate that the large amplitude part of the distribution dominates the gravitational wave signal.

### B. Results

In Fig. 6 we plot $\log Q_1^{1/4}(n)$ as a function of the generation $n$, for different sets of string tensions $\mu_1$, $\mu_2$ and $\mu_3$. (The particular choice of $A = 1/4$ will be justified in [19].) The initial condition at the start of the simulation was a single right-moving kink $K = 1$ of maximal amplitude on each string.

After some initial fluctuations at small $n$, which vary significantly from one realization to another [35], one sees that the points corresponding to a given set of string tensions can be fitted to a straight line, whose slope is independent of the particular realization. Hence $Q_1^{1/4}(n)$ grows exponentially with $n$. More generally we find [36]

$$Q_j^A(n) \propto \exp[\gamma n], \tag{32}$$

where the coefficient $\gamma$ depends on the tensions $\mu_j$ as well as on the amplitude $A$. One sees proliferation is most efficient when all tensions are equal. Gradually moving away from this case, the slope $\tilde{\gamma} = \gamma/\ln(10)$ of the curves in Fig. 6 decreases and approaches zero when one or more of the $\nu_j$ given in (5) vanish. For a given ratio of tensions, we find $\gamma$ is approximately independent of $A$ over most of the range of possible amplitudes. For equal tensions and

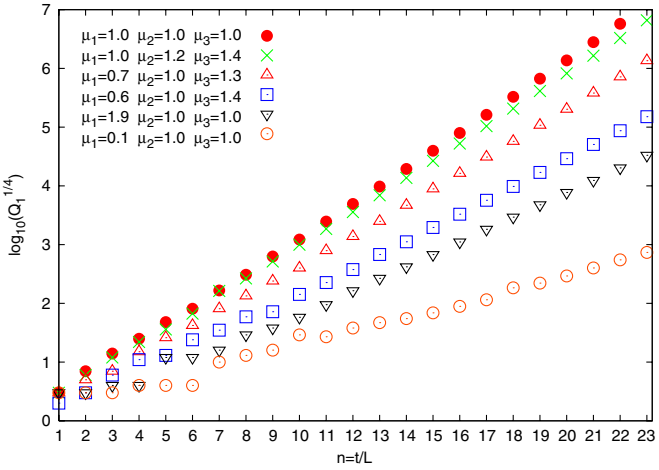


FIG. 6 (color online). The logarithm of the number of kinks on string 1 of amplitude $A \geq 1/4$, as a function of time measured in units of the constant string length $L$, for different sets of string tensions $\mu_1$, $\mu_2$ and $\mu_3$.

$A \geq 0.1$ shown in Fig. 6 one has $\tilde{\gamma} \approx 1/3$. In the limit $A \to 0$, the slope sharply increases to $\gamma \approx \ln 3$, since obviously $Q_j^0(n) = 3^n$.

We therefore conclude that, at least in this simplified model of a loop with junctions, for a large range of string tensions, the amplification rate is sufficient to sustain an exponential growth of the number of large amplitude kinks. In Appendix B we illustrate, with a toy analytical model, the origin of this exponential growth. We must emphasize, however, that since amplification remains a rare event, the vast majority of kinks at sufficiently late times will have small amplitude. Indeed, the fraction of the total number of kinks that have a large amplitude tends to zero. The implications of these findings for the gravitational wave signal emitted by string loops of this kind will be studied elsewhere [19].

## V. PROLIFERATION OF LARGE AMPLITUDE KINKS ON EVOLVING LOOPS WITH JUNCTIONS

The model of a loop with junctions discussed in Sec. IV does not take in account the dynamics of the loop. In particular, it assumes the invariant length of the strings forming the loop is constant in time. Here we include the effects of the loop dynamics on the evolution of the number of large amplitude kinks, by numerically integrating the equations of motion (9) and (10), suitably modified to take account of the presence of the two junctions.

This is more complicated than for periodic loops with no junctions, since one needs to keep track of the position of each junction, and extend the definition of the $\mathbf{a}_j'$ beyond their initial domain. Our simulations generalize those of [28] in which certain initially static and symmetric planar loop configurations were studied. Here we consider a rather general class of nonstatic initial conditions, and count the number as well as the amplitude of the kinks on the loop as a function of time. Note, however, that we do not take in account self-intersections between the strings in our simulations. This may be an important limitation of our model if the probability of intercommutation is large. (In this case, intercommutation between strings of the same type would lead to a loop being chopped off, whereas intercommutation between strings of different types might increase the number of junctions in the loop.) Our simulations end when the length of one of the strings connecting the two junctions shrinks to zero and the junctions collide. The outcome of such a collision is an open question, but it may well lead to the formation of two loops without junctions (assumed, e.g., in [37]): this would end the proliferation of kinks.

### A. Initial conditions

Our initial condition consists of 3 segments of string of initial invariant length $L_j(t = 0)$ (specified below) which join two junctions at positions

$$\mathbf{X}_A = (0, 0, -1), \qquad \mathbf{X}_B = (0, 0, 1). \tag{33}$$

Motivated by the harmonic construction of standard cosmic string loops with no junctions [38–42], the three initial string segments are taken to be three arcs of circles to which we add a higher harmonic. Explicitly,

$$\mathbf{x}_j(\sigma, t = 0) = \mathcal{R}(\alpha_j)\begin{pmatrix} -\sin\left(\frac{\sigma}{H_j}\right)\left[1 + a_j \sin\left(m_j \frac{\sigma}{H_j}\right)\right] \\ 0 \\ \cos\left(\frac{\sigma}{H_j}\right)\left[1 + b_j \sin\left(n_j \frac{\sigma}{H_j}\right)\right] \end{pmatrix}, \tag{34}$$

where $m_j, n_j \in \mathbf{N}$, and $\mathcal{R}(\alpha_j)$ is the rotation matrix about the $z$ axis by an angle $\alpha_j$

$$\mathcal{R}(\alpha_j) = \begin{pmatrix} \cos(\alpha_j) & -\sin(\alpha_j) & 0 \\ \sin(\alpha_j) & \cos(\alpha_j) & 0 \\ 0 & 0 & 1 \end{pmatrix}. \tag{35}$$

If we set $a_j = b_j = 0$, then the segments are initially semicircles. If $a_j$ or $b_j$ are nonzero then the strings appear as perturbed semicircles (at least for small values of $a_j$ and $b_j$), and the integers $m_j$ and $n_j$ set the "wiggliness" of the perturbation. The normalization

$$H_j = \sqrt{(1 + a_j)^2 + (a_j m_j)^2 + (1 + b_j)^2 + (b_j n_j)^2} \tag{36}$$

ensures that $\|\mathbf{x}_j'\| \leq 1$ since $\dot{\mathbf{x}}_j^2 + \mathbf{x}_j'^2 = 1$ from the gauge conditions (2). Note that with this definition of $H_j$ in general $\sup\|\mathbf{x}_j'\| < 1$ so that the initial condition is never static. The initial invariant length of the strings segments is $L_j(0) = \pi H_j$ so that

$$\sigma \in [-\pi H_j, 0] \quad \text{at } t = 0. \tag{37}$$

In order to compare our results with Sec. IV, we will measure time in units of

$$L = \frac{1}{3}(L_1(t) + L_2(t) + L_3(t)), \tag{38}$$

the total invariant length of the loop divided by the number of string segments. Note that this quantity remains constant throughout the evolution.

The initial velocity of the strings $\dot{\mathbf{x}}_j$ must satisfy the gauge condition $\dot{\mathbf{x}}_j \cdot \mathbf{x}_j' = 0$. We choose it to be

$$\dot{\mathbf{x}}_j(\sigma, t = 0) = N_j(\sigma)\mathcal{R}(\alpha_j)\begin{pmatrix} \sin\left(\frac{\sigma}{H_j}\right)\left(1 + b_j \sin\left(n_j \frac{\sigma}{H_j}\right)\right) - b_j n_j \cos\left(\frac{\sigma}{H_j}\right)\cos\left(n_j \frac{\sigma}{H_j}\right) \\ \upsilon_j \\ -\cos\left(\frac{\sigma}{H_j}\right)\left(1 + a_j \sin\left(m_j \frac{\sigma}{H_j}\right)\right) - a_j m_j \sin\left(\frac{\sigma}{H_j}\right)\cos\left(m_j \frac{\sigma}{H_j}\right) \end{pmatrix}, \tag{39}$$

with $N_j(\sigma)$ defined so that $\dot{\mathbf{x}}_j^2 = 1 - \mathbf{x}_j'^2$, and $\upsilon_j$ is the component of velocity transverse to the plane of the string. Finally the functions $\mathbf{a}_j'(z)$ and $\mathbf{b}_j'(z)$ on the interval $[-\pi H_j, 0]$ are obtained through

$$\mathbf{a}_j'(z) = \mathbf{x}_j'(\sigma = z, t = 0) + \dot{\mathbf{x}}_j(\sigma = z, t = 0), \tag{40}$$

$$\mathbf{b}_j'(z) = \mathbf{x}_j'(\sigma = z, t = 0) - \dot{\mathbf{x}}_j(\sigma = z, t = 0). \tag{41}$$

As explained in Sec. II, the $\sigma$ parameter on each string takes values in $[s_{A,j}(t), s_{B,j}(t)]$ at time $t$. Furthermore, integrating the equations of motion extends the definition of the functions $\mathbf{a}_j'(z)$ and $\mathbf{b}_j'(z)$ outside the interval $[-\pi H_j, 0]$ [using Eqs. (10)] to $z > 0$ for $\mathbf{a}_j'(z)$ and to $z < -\pi H_j$ for $\mathbf{b}_j'(z)$. Thus if the evolution is calculated up to a final time $t_f$, then at the end of the simulation $\mathbf{a}_j'(z)$ will be defined in the interval $[-\pi H_j, z_{f,j}]$ where $z_{f,j} = t_f + s_{B,j}(t_f)$.

### B. Proliferation of large amplitude kinks

This class of initial conditions has 6 parameters for each string: $\alpha_j$, $a_j$, $b_j$, $m_j$, $n_j$ and $\upsilon_j$, and therefore enables one to probe a variety of initial configurations. We now evolve these strings and count the number of large amplitude kinks as a function of time. That is, we calculate $A[\mathbf{a}_j'](z) = \frac{1}{2}\|\mathbf{a}_j'(z^+) - \mathbf{a}_j'(z^-)\|$ (for left-moving kinks) and $A[\mathbf{b}_j'](z) = \frac{1}{2}\|\mathbf{b}_j'(z^+) - \mathbf{b}_j'(z^-)\|$ as functions of $z$. These functions are zero except at the position of a kink, where they reduce to the kink amplitude.

As discussed in Sec. II, even though the initial configuration is infinitely smooth and appears to contain no kinks, this is not the case. While $\mathbf{a}_j'$ and $\mathbf{b}_j'$ are continuous inside the interval $]-\pi H_j, 0[$ they have a discontinuity at $z = -\pi H_j$ for $\mathbf{b}_j'(z)$ and $z = 0$ for $\mathbf{a}_j'(z)$. Indeed, as soon as the evolution starts, the equations of motion define the function $\mathbf{a}_j'(z)$ for $z > 0$. In particular, $\mathbf{a}_j'(z = 0^+)$ depends only on the values of the $\mathbf{b}_\ell'(z = 0^-)$ for $\ell = 1, 2, 3$ and differs from $\mathbf{a}_j'(z = 0^-)$. Our loop therefore initially contains 6 kinks: one left-moving and one right-moving on each string of the loop.

The numerical integration of the equations of motion ends at time $t_f$ when the two junctions collide. The results are shown in Fig. 7 for the case of equal tension strings $\mu_j = 1$. Here we have used the following set of parameters as initial conditions: string 1 ($\alpha_1 = 0, A_1 = 0.2, B_1 = 0.3, m_1 = 2, n_1 = 3, \upsilon_t = 0$), string 2 ($\alpha_2 = 2\pi/3, A_2 = 0.1, B_2 = 0.2, m_2 = 3, n_2 = 4, \upsilon_t = 0$) and

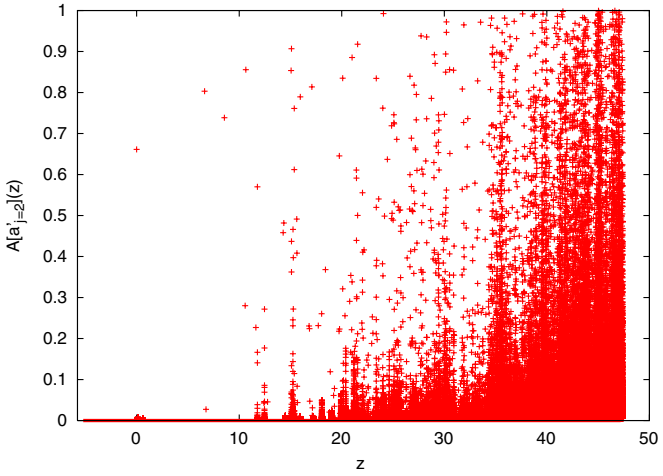


FIG. 7 (color online). $A[\mathbf{a}'_{j=2}](z)$ as a function of $z$. We evolved until $t_f = 50$ which corresponds to $z_{f,2} = 47.4$. Each point above zero corresponds to a left-moving kink propagating on string number 2. As the system evolves, many kinks are created, and although the vast majority has a very small amplitude, a large number has an amplitude of the order of 1.

string 3 ($\alpha_3 = 4\pi/3$, $A_3 = 0.2$, $B_3 = 0.4$, $m_3 = 1$, $n_3 = 3$, $v_t = 0$). A snapshot of this loop shortly after the beginning of the simulation is shown in Fig. 5. One can see the six kinks propagating away from the junctions.

As one can see in Fig. 7 the total number of (left-moving) kinks that have propagated on string number 2 is very large, and even though the amplitude of many of those kinks is small there still is a large number of those kinks with an amplitude larger than, e.g., $1/4$. This is in line with the results in the previous section. We can be more precise by calculating $Q_j^{1/4}$, the number of (left-moving) kinks

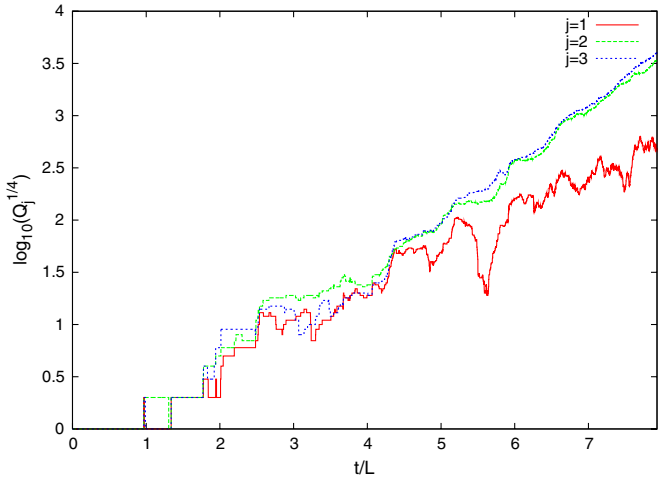


FIG. 8 (color online). The logarithm of the number of (left-moving) kinks of amplitude $A \geq 1/4$ on each string, as a function of time measured in units of the total invariant length of the loop $L$ defined in (38) (which remains constant in time), for the case of strings with equal tensions. After some initial fluctuations, a regime of exponential growth sets in.

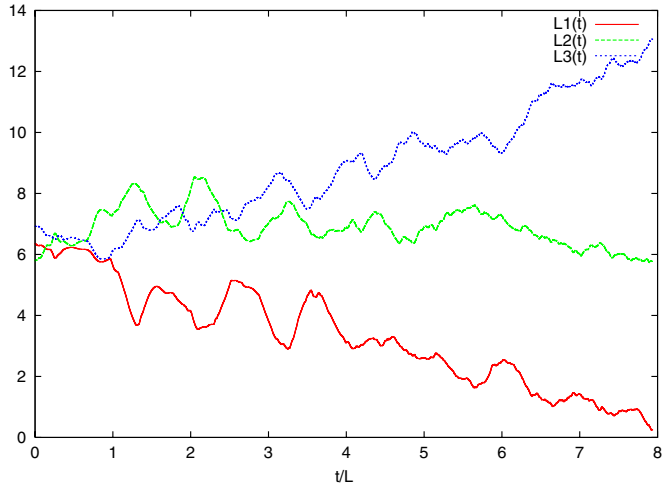


FIG. 9 (color online). Evolution of the "invariant lengths" of the strings. The simulations end around $t_f = 50$ when string 1 shrinks to a point and the junctions collide.

propagating on string $j$ with an amplitude larger than $1/4$, as a function of time measured in units $L$ defined in (38). The result is shown in Fig. 8. One clearly sees that after some initial fluctuations, a regime of exponential growth sets in.

Remarkably, the slope of the curves in Fig. 8 is larger than the slope of the corresponding function $\log Q_j^{1/4}$, shown in Fig. 6 for the simple model of a loop with junctions discussed in Sec. IV (where we do not take in account the loop evolution). The reason that loop dynamics has this effect on the proliferation process is simply because the loop dynamics generally implies that one of the strings shrinks. On this string, kinks propagate more frequently backward and forward between the junctions, thereby increasing the rate of proliferation. One expects therefore that, for a given set of tensions, proliferation is in fact the least efficient when all lengths are constant and equal, which is just the case considered in Sec. IV, and that the rate obtained here is more realistic. We note when the string that is shrinking becomes small, kinks tend to have a smaller amplitude on it.

Finally, we note that these simulations end at $t_f = 50$ because the junctions collide briefly after that time, as is evident from Fig. 9. At that time, the total number of kinks on this loop is of the order $10^4$.

### C. Discussion

The details of the evolution of the number of kinks evidently depend somewhat on the initial conditions. However, our central result that the number of large amplitude kinks proliferates exponentially appears to be universal. In particular, it is a robust feature of the evolution for the wide range of parameter values we have scanned.

The loop evolution has two important implications for the evolution of kinks. First, as discussed above, it

enhances the proliferation rate because the length of one of the strings generally decreases. On this string, kinks propagate more frequently backward and forward between the junctions.

However, at the same time this possibly provides an end to the proliferation process. Indeed, for all the initial conditions that we have tried, one of the strings always ended up shrinking to a point, resulting in the collision of the two junctions. The result of such a collision is unclear and depends on the physics of the underlying theory [28]. The junctions might disappear thus ending the proliferation, or two new junctions might form and proliferation may then continue.

Gravitational backreaction (e.g., by rounding off the kinks or by inducing the decay of the loop due to important radiation from the many kinks) may also end the proliferation. Finally, radiation of other fields might also become important as the number of kinks increases and could also play a limiting role.

## VI. CONCLUSION

Motivated by their effects on the gravitational wave emission of cosmic strings and superstrings, we have studied the dynamics of kinks on strings with junctions [43]. We have concentrated, in particular, on the evolution of the number of very sharp—or equivalently, large amplitude—kinks since it turns out these provide the dominant contribution to the GW burst signal from kinks on a network of strings [19].

The propagation of a kink through a $Y$ junction leads to the formation of three daughter kinks—one reflected kink and two transmitted kinks. We first showed analytically that, for a specific initially static junction configuration, one or two of the daughter kinks can be sharper than the incoming kink. This turns out not to be an isolated case: the amplification of kinks through their interaction with junctions is a rather generic phenomenon. Indeed we showed in Sec. III that, assuming a random distribution for the four incoming waves specifying the junction configuration and for equal string tensions, kinks are amplified in a significant region of configuration space. In Appendix A we have generalized this calculation to strings of different tensions finding similar results.

The dominant contribution to the GW signal from a network of strings comes from the loops. In Secs. IV and V we have therefore studied the evolution of kinks on loops with junctions. We have considered loops which, for simplicity, contain 2 junctions. If one neglects the loop dynamics and assumes that (i) all strings joining the two junctions have essentially the same invariant length, and also that (ii) when a kink of known amplitude reaches a junction, the configuration of the latter is randomly drawn among those that yield the correct amplitude for the original kink, then one finds the amplification rate is sufficient to sustain an exponential growth of the number of large amplitude kinks. For a wide range of tensions, the coefficient in the exponent appears to be of order 1 when time is measured in units of $L$. The origin of this exponential growth was illustrated with a toy model in Appendix B.

We have included the effect of the loop dynamics on the proliferation and amplification of kinks in Sec. V, where we numerically integrated the equations of motion of a loop with two junctions for a rather general class of initial conditions. Our simulations generalize those of [28], which considered an initially static and symmetric planar loop configuration. Interestingly, we find the loop evolution somewhat enhances the rate at which the number of large amplitude kinks grows. To a large extent this difference can be traced to the fact that under evolution, generically one of the strings shrinks. On this string, kinks propagate more frequently backward and forward between the junctions, thereby increasing the rate of proliferation and thus also the number of large amplitude kinks. By the time the junctions on the loop collide we typically find at least as many as $\sim 10^4$ large amplitude kinks in the equal tension case.

We note, however, that our simulations do not take into account intercommutations between strings. These may lead to the creation of new junctions as well as several smaller loops (with many kinks). Further, we end our simulations just before the junctions collide and have not addressed the subsequent evolution of the system. Finally, we note that backreaction effects will become increasingly important as the number of kinks grows, and that our simulations do not include this effect.

Nevertheless our findings suggest that if an evolving network of strings with junctions contains a population of loops with junctions, these typically contain a large number of very sharp kinks. The implications of this for the GW signal emitted by networks of this kind will be discussed elsewhere [19].

## ACKNOWLEDGMENTS

D. A. S. thanks Tom Kibble, Hassan Firouzjahi, Christophe Ringeval and Tanmay Vachaspati for useful comments and discussions. This work was supported by the Agence Nationale de la Recherche grant "STR-COSMO" (ANR-09-BLAN-0157).

## APPENDIX A

In this appendix we study the dependence of the distributions $p(C_j)$ of transmission coefficients on the ratios of the tensions of each of the strings, for three semi-infinite strings meeting at a junction. The case of equal tensions was discussed in the text in Sec. III where it was found that the distributions of both the reflected and the transmitted kinks have significant tails where $C_j > 1$. As in Sec. III, we consider a kink moving towards the junction on string 1 and assume a uniform distribution on the unit sphere of the vectors $\mathbf{b}'_j$ that specify the junction configuration.

### 1. Incoming kink on a light string: $\mu_1 \ll \mu_2 \sim \mu_3$

The kink reaches the junction on a string which is much lighter than the other two strings. One might therefore expect, on average, the kinks transmitted to the heavier strings to have reduced amplitudes and the reflected kink to have an amplitude comparable or even enhanced relative to the amplitude of the incoming kink.

This is indeed what we find. Figure 10 shows the marginal distributions $p(C_j)$ for strings of tensions $\mu_1 = 0.1$, $\mu_2 = \mu_3 = 1$. One sees the distribution of $C_1$ is relatively flat, with a probability of amplification $P(C_1 > 1)$ larger than 10 percent. On the other hand $p(C_2)$ is sharply peaked around a value much smaller than 1.

The existence of this peak can be understood from Eq. (27). Let $\epsilon = \mu_1/\mu \ll 1$ and take $\mu_2 \sim \mu_3$ so that $\nu_1/\mu \sim O(\epsilon)$. Then from (8) it follows that $\dot{s}_2^{\pm} + \dot{s}_3^{\pm} = O(\epsilon)$ so that

$$\mathbf{a}_2'^{\pm} = \left(\frac{1-\dot{s}_2^{\pm}}{1+\dot{s}_2^{\pm}}\right)\underbrace{\left(\frac{\nu_1}{\mu}\right)}_{O(\epsilon)}\mathbf{b}_2' - \underbrace{\left(\frac{2\mu_3}{\mu}\right)}_{1+O(\epsilon)}\underbrace{\frac{1-\dot{s}_3^{\pm}}{1+\dot{s}_2^{\pm}}}_{1+O(\epsilon)}\mathbf{b}_3' - \underbrace{\frac{2\mu_1}{\mu}}_{O(\epsilon)}\frac{1-\dot{s}_1^{\pm}}{1+\dot{s}_2^{\pm}}\mathbf{b}_1'^{\pm}. \tag{A1}$$

Now generically one has $1 - \dot{s}_2^{\pm} \sim O(\epsilon)$ for the above configuration of tensions [32]. Therefore, since the functions $\mathbf{b}_2'$ and $\mathbf{b}_3'$ do not change when the kink crosses the junctions, it follows that

$$A[\mathbf{a}_2'] = \frac{1}{2}\|\mathbf{a}_2'^{-} - \mathbf{a}_2'^{+}\| \sim O(\epsilon)A[\mathbf{b}_1'] \Rightarrow C_2 \sim O(\epsilon). \tag{A2}$$

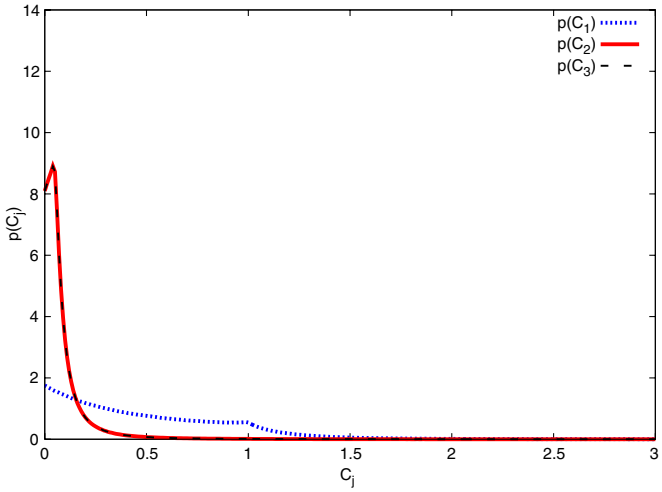


FIG. 10 (color online). Distributions of the different transmission coefficients for tensions $\mu_1 = 0.1$, $\mu_2 = \mu_3 = 1$, with the incoming kink on string 1. The average values are $\langle C_1\rangle = 0.49$, $\langle C_2\rangle = \langle C_3\rangle = 0.09$ and $P(C_1 < 1) = 0.88$, $P(C_2 < 1) = P(C_3 < 1) = 0.99$.

The coefficient $C_2$ will be large only if either $\dot{s}_2^{+}$ or $\dot{s}_2^{-}$ is close to minus one. However, the probability for this is small; according to [32] only three percent of the $\dot{s}_2^{\pm}$ lie in the interval $[-1, -0.9]$, which explains why very few events are seen in the tail at large values of the distributions of $C_2$ and $C_3$.

Finally, the average values of the transmission coefficients for the above set of tensions are given by

$$\langle C_1\rangle = 0.49, \qquad \langle C_2\rangle = \langle C_3\rangle = 0.09. \tag{A3}$$

### 2. Incoming kink on a heavy string: $\mu_1 \sim \mu_3 \gg \mu_2$

In this case, the kink propagates on a heavy string towards a junction consisting of another heavy string as well as a very light one. The light string is expected to play a minor role while the heavy strings almost behave as a single long string without junction on which the kink simply propagates. Hence the reflected kink amplitude $C_1$ should be peaked at a very small value, while the transmitted kink amplitude on the heavy string $C_3$ should be peaked at 1. This is indeed what we find, as shown in Fig. 11), and an analytic argument similar to the one given above can be used to explain the position of the peaks in the distributions [46] of $C_1$ and $C_2$.

We now have $\dot{s}_1 + \dot{s}_3 = O(\epsilon)$. The argument for $C_1$ is exactly the same as above, since

$$\mathbf{a}_1' = \frac{1-\dot{s}_1}{1+\dot{s}_1}\underbrace{\left(1 - \frac{2\mu_1}{\sum_k \mu_k}\right)}_{O(\epsilon)}\mathbf{b}_1' - \underbrace{\frac{2\mu_2}{\sum_k \mu_k}}_{O(\epsilon)}\frac{1-\dot{s}_2}{1+\dot{s}_1}\mathbf{b}_2' - \underbrace{\frac{2\mu_3}{\sum_k \mu_k}}_{1+O(\epsilon)}\underbrace{\frac{1-\dot{s}_3}{1+\dot{s}_1}}_{1+O(\epsilon)}\mathbf{b}_3'. \tag{A4}$$

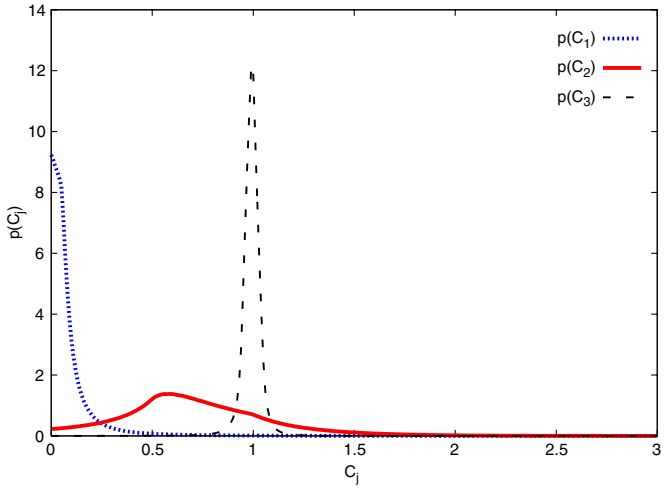


FIG. 11 (color online). The same distributions as in Fig. 10 but for tensions $\mu_1 = 1$, $\mu_2 = 0.1$ and $\mu_3 = 1$. Here $\langle C_1\rangle = 0.09$, $\langle C_2\rangle = 0.72$, $\langle C_3\rangle = 0.99$ and $P(C_1 < 1) = 0.99$, $P(C_2 < 1) = 0.81$, $P(C_3 < 1) = 0.53$.

For $C_3$, we have

$$\mathbf{a}_3' = \frac{1-\dot{s}_3}{1+\dot{s}_3}\underbrace{\left(1-\frac{2\mu_3}{\sum_k \mu_k}\right)}_{O(\epsilon)}\mathbf{b}_3' - \underbrace{\frac{2\mu_2}{\sum_k \mu_k}}_{O(\epsilon)}\frac{1-\dot{s}_2}{1+\dot{s}_3}\mathbf{b}_2' - \underbrace{\frac{2\mu_1}{\sum_k \mu_k}}_{1+O(\epsilon)}\underbrace{\frac{1-\dot{s}_1}{1+\dot{s}_3}}_{1+O(\epsilon)}\mathbf{b}_1'. \tag{A5}$$

The zeroth order in $\epsilon$ does not vanish in $\Delta\mathbf{a}_3'$, because $\mathbf{b}_1'$ undergoes a jump. Instead we have, in generic configurations where the other coefficients are of order 1, $\Delta\mathbf{a}_3' \approx \Delta\mathbf{b}_1'$ which means $C_3 \approx 1$.

The mean values $\langle C_j\rangle$ for the set of tensions of Fig. 11 are smaller than 1,

$$\langle C_1\rangle = 0.09, \qquad \langle C_2\rangle = 0.72, \qquad \langle C_3\rangle = 0.99, \tag{A6}$$

but the probability of having an amplification on strings 2 and 3 is significant,

$$P(C_1 > 1) = 0.01, \qquad P(C_2 > 1) = 0.19, \qquad P(C_3 > 1) = 0.47. \tag{A7}$$

Again we note that, for string 3, although amplification is frequent this is mostly limited in amplitude since the distribution is sharply peaked around a value close to 1.

An analytic string theory calculation of the transmission of short pulses at a junction between two $D$ strings and an $F$ string in the weak coupling limit can be found in [47].

### 3. Incoming kink on a heavy string with $\mu_1 \lesssim \mu_2 + \mu_3$

In the example shown in Fig. 12, $\mu_2 = \mu_3 = 1$ and $\mu_1 = 1.9$. The (superimposed) distributions $p(C_2)$, $p(C_3)$ are sharply peaked around 1, so the amplitude of the kinks transmitted to the light strings is comparable to that of the incoming kink on the heavy string. The distribution of $C_1$ is much flatter, with a significant tail at large values. For this set of tensions one has

$$P(C_1 > 1) = 0.11. \tag{A8}$$

The presence and position of the peak in $p(C_2)$ can again be explained using an analytic argument. Let $\epsilon = \frac{\nu_1}{\mu} \ll 1$. For most configurations, one has $\dot{s}_1^{\pm} = -1 + O(\epsilon)$, while $\dot{s}_2^{\pm} = 1 - O(\epsilon)$ and $\dot{s}_3^{\pm} = 1 - O(\epsilon)$ [32] [see also (9)]. Thus from Eq. (27),

$$\mathbf{a}_2'^{\pm} = \underbrace{\frac{1-\dot{s}_2^{\pm}}{1+\dot{s}_2^{\pm}}}_{O(\epsilon)}\left(\frac{\nu_2}{\mu}\right)\mathbf{b}_2' - \frac{2\mu_3}{\mu}\underbrace{\frac{1-\dot{s}_3^{\pm}}{1+\dot{s}_2^{\pm}}}_{O(\epsilon)}\mathbf{b}_3' - \underbrace{\frac{2\mu_1}{\mu}}_{1+O(\epsilon)}\underbrace{\frac{1-\dot{s}_1^{\pm}}{1+\dot{s}_2^{\pm}}}_{1+O(\epsilon)}\mathbf{b}_1'^{\pm}. \tag{A9}$$

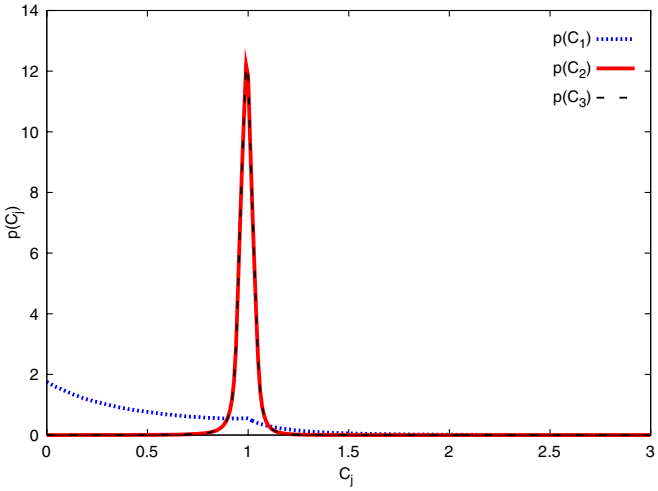


FIG. 12 (color online). Distributions of the different transmission coefficients for tensions $\mu_1 = 1.9$ and $\mu_2 = 1 = \mu_3$. The mean values are $\langle C_1\rangle = 0.49$, $\langle C_2\rangle = 0.99$, $\langle C_3\rangle = 0.99$ and $P(C_1 < 1) = 0.88$, $P(C_2 < 1) = 0.53$, $P(C_3 < 1) = 0.53$.

Hence to zeroth order in $\epsilon$, $\Delta\mathbf{a}_2' \approx \Delta\mathbf{b}_1'$ and therefore $C_2 \approx 1$. A similar argument applies to $C_3$.

### 4. Incoming kink on light string of tension $\mu_1 \gtrsim \mu_2 - \mu_3$

Finally in Fig. 13, we show the distributions of the transmission coefficients for the following set of tensions: $\mu_1 = \mu_3 = 1$ and $\mu_2 = 1.9$. One sees $p(C_1)$ and $p(C_3)$ are peaked at small values. The typical amplitude of the kinks reflected on the light string $\mu_1$ and transmitted on the other light string of tension $\mu_3$ is very small. The distribution of $C_2$ is flatter, so the amplitude of the kink transmitted to the heavy string depends strongly on the configuration. This

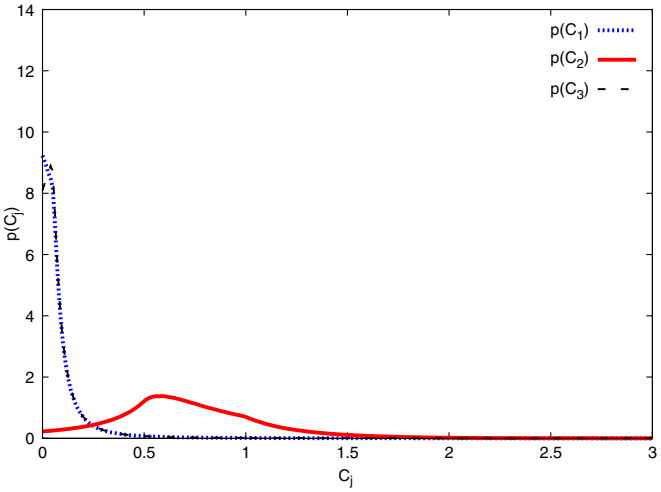


FIG. 13 (color online). The same distributions as in Fig. 12 for tensions $\mu_1 = 1 = \mu_3$ and $\mu_2 = 1.9$. Here $\langle C_1\rangle = 0.09$, $\langle C_2\rangle = 0.72$, $\langle C_3\rangle = 0.99$ and $P(C_1 < 1) = 0.99$, $P(C_2 < 1) = 0.81$, $P(C_3 < 1) = 0.99$.

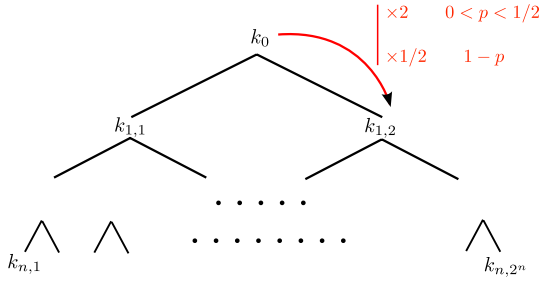


FIG. 14 (color online). Random experiment described in this section.

distribution also has a tail for $C_2 > 1$, so kinks are amplified in a substantial volume of configuration space:

$$P(C_2 > 1) = 0.19. \tag{A10}$$

Again the presence and the position of the peak in $p(C_1)$ and $p(C_3)$ can be explained analytically. The argument is as above though now $\epsilon = \frac{\nu_2}{\mu} \ll 1$ and, in most configurations, $\dot{s}_1 = 1 - O(\epsilon)$ and $\dot{s}_3 = 1 - O(\epsilon)$ while $\dot{s}_2 = -1 + O(\epsilon)$.

## APPENDIX B

Here we illustrate with a very simple toy model that an exponential behavior of the kind exhibited in Secs. IV and V is actually very generic.

Consider the situation illustrated in Fig. 14 in which one constructs a tree, in which each node has two daughter nodes so that the $n$th generation therefore contains $2^n$ nodes. Each node contains an amplitude and the amplitude of each of its daughter nodes is obtained by multiplying this amplitude by a factor drawn randomly using a Bernoulli distribution: 2 with probability $p$ or $1/2$ with probability $1 - p$. This means that there is either an amplification (by a factor of 2) or a reduction of amplitude (by a factor of $1/2$). Since we are interested in the case where amplifications are the least probable outcome, we set

$$p < 1/2. \tag{B1}$$

In order to initialize the experiment, we need to define the amplitude of the initial node (0th generation): we set it to be 1.

Let $p_n$ be the probability that any given node of the $n$th generation (say, $k_{1,n}$ for instance) has an amplitude larger than 1. Since $p < 1/2$, we expect $p_n$ to be small when $n$ becomes large. Our goal here is to compute analytically (in the large $n$ limit) $p_n$.

In order to be larger than 1, $k_{1,n}$ must be the result of more amplifications than reductions so we clearly have

$$p_n = \sum_{k \geq n/2} \binom{n}{k} p^k (1-p)^{n-k}. \tag{B2}$$

Using Stirling's formula and transforming the sum into an integral using $x = k/n$, we can easily obtain

$$p_n = \sqrt{n} \int_{1/2}^{1} \frac{1}{\sqrt{x(1-x)}} e^{n f_p(x)} dx \tag{B3}$$

with

$$f_p(x) = -x \ln\left(\frac{x}{p}\right) - (1-x) \ln\left(\frac{1-x}{1-p}\right). \tag{B4}$$

In the interval $[1/2, 1]$, $f_p(x)$ is a decreasing function (because $p < 1/2$), and therefore, it is maximal for $x = 1/2$. Because of the exponential in the integral, we then expect the dominant contribution to $p_n$ to come from the vicinity of $1/2$. More precisely, by computing carefully the integral, it is possible to show that

$$p_n \underset{n \to +\infty}{\sim} \frac{2}{-f_p'(1/2)} \frac{\sqrt{n}}{n} e^{n f_p(1/2)} \tag{B5}$$

$$= \frac{2}{\ln(\frac{1-p}{p})} \frac{1}{\sqrt{n}} (2\sqrt{p(1-p)})^n. \tag{B6}$$

As expected, $p_n$ decreases exponentially since $2\sqrt{p(1-p)} < 1$. However, we are interested in the number $N_n$ of nodes of the $n$th generation that have an amplitude larger than 1. If $n$ is large enough, this number will typically be $2^n p_n$:

$$N_n \underset{n \to +\infty}{\sim} \frac{2}{\ln(\frac{1-p}{p})} \frac{1}{\sqrt{n}} (4\sqrt{p(1-p)})^n. \tag{B7}$$

This number increases exponentially when $4\sqrt{p(1-p)} > 1$, i.e., $p(1-p) > \frac{1}{16}$. This condition is satisfied as soon as $p > \frac{1}{2} - \frac{\sqrt{3}}{4} \approx 0.07$ (remember that we also imposed $p < 1/2$).

This means that even if amplifications are not the most probable outcome of amplitude transmissions (as is the case for our physical system), the number of nodes of the $n$th generation that have an amplitude larger than some fixed value increases exponentially provided that $p$ is not too small, i.e., provided that amplifications are not too rare.

Note that the fraction of nodes that have an amplitude larger than 1 is given by $p_n$ and tends to 0 exponentially fast and that the proliferation of large amplitude nodes is only possible because the total number ($2^n$ in our example) increases faster than $p_n$ decreases. As expected, the very large majority of nodes have small amplitude.

Of course, this very simple example is not a good physical picture of our kink proliferation (amplitudes can be larger than 1 in this example). Indeed, the Bernoulli distribution is a crude simplification of $p_{A_i}(C_1, C_2, C_3)$ which does not take into account the fact that the amplitudes of the daughter kinks are actually correlated and forgets about the amplitude of the incoming kink $A_i$. However, we expect the general mechanism to remain the same.

[1] J. Polchinski, in *The New Cosmology: Conference on Strings and Cosmology; The Mitchell Symposium on Observational Cosmology*, edited by R. E. Allen, D. V. Nanopoulos, and C. N. Pope, AIP Conf. Proc. No. 743 (AIP, New York, 2005), p. 331; Int. J. Mod. Phys. A **20**, 3413 (2005).

[2] T. W. B. Kibble, arXiv:astro-ph/0410073.

[3] A. C. Davis and T. W. B. Kibble, Contemp. Phys. **46**, 313 (2005).

[4] R. C. Myers and M. Wyman, in *String Cosmology*, edited by J. Erdmenger, (Wiley, Berlin, 2009), p. 121.

[5] E. J. Copeland and T. W. B. Kibble, Proc. R. Soc. A **466**, 623 (2010).

[6] S. H. Tye, I. Wasserman, and M. Wyman, Phys. Rev. D **71**, 103508 (2005); **71**, 129906(E) (2005).

[7] M. Hindmarsh and P. M. Saffin, J. High Energy Phys. 08 (2006) 066.

[8] E. J. Copeland and P. M. Saffin, J. High Energy Phys. 11 (2005) 023.

[9] J. Urrestilla and A. Vilenkin, J. High Energy Phys. 02 (2008) 037.

[10] A. Avgoustidis and E. P. S. Shellard, Phys. Rev. D **78**, 103510 (2008); **80**, 129907(E) (2009).

[11] A. Avgoustidis and E. J. Copeland, Phys. Rev. D **81**, 063517 (2010).

[12] T. Damour and A. Vilenkin, Phys. Rev. D **71**, 063510 (2005).

[13] X. Siemens, J. Creighton, I. Maor, S. Ray Majumder, K. Cannon, and J. Read, Phys. Rev. D **73**, 105001 (2006).

[14] X. Siemens, V. Mandic, and J. Creighton, Phys. Rev. Lett. **98**, 111101 (2007).

[15] M. G. Jackson and X. Siemens, J. High Energy Phys. 06 (2009) 089.

[16] M. G. Jackson, N. T. Jones, and J. Polchinski, J. High Energy Phys. 10 (2005) 013.

[17] E. J. Copeland, T. W. B. Kibble, and D. A. Steer, Phys. Rev. Lett. **97**, 021602 (2006).

[18] E. J. Copeland, H. Firouzjahi, T. W. B. Kibble, and D. A. Steer, Phys. Rev. D **77**, 063521 (2008).

[19] P. Binetruy, A. Bohe, T. Hertog, and D. A. Steer (unpublished).

[20] Note that spontaneous symmetry breaking phase transitions can also lead to the formation of cosmic strings with junctions, and hence our analysis also applies to such strings.

[21] M. DePies and C. Hogan, Phys. Rev. D **75**, 125006 (2007).

[22] T. Damour and A. Vilenkin, Phys. Rev. D **64**, 064008 (2001).

[23] P. Binetruy, A. Bohe, T. Hertog, and D. A. Steer, Phys. Rev. D **80**, 123510 (2009).

[24] A. C. Davis, W. Nelson, S. Rajamanoharan, and M. Sakellariadou, J. Cosmol. Astropart. Phys. 11 (2008) 022.

[25] E. O'Callaghan, S. Chadburn, G. Geshnizjani, R. Gregory, and I. Zavala, Phys. Rev. Lett. **105**, 081602 (2010).

[26] Kink amplitude, defined in Sec. III, is synonymous with the kink sharpness—a nomenclature often used elsewhere.

[27] The exception is when, given the $\mathbf{b}'_j(s_j(0)^-)$, the $\mathbf{a}'_j(s_j(0)^-)$ are chosen to be given by the right-hand side of Eq. (10). A particular case of this is totally static initial conditions ($\dot{\mathbf{x}}_j = 0 = \dot{\mathbf{X}} = \dot{s}_j$) considered in [28].

[28] N. Bevis, E. J. Copeland, P. Y. Martin, G. Niz, A. Pourtsidou, P. M. Saffin, and D. A. Steer, Phys. Rev. D **80**, 125030 (2009).

[29] The energy along the string is proportional to $\sigma$. Hence no energy is associated to the kink itself which is described by a pointlike discontinuity.

[30] We only plot $C_1$ and $C_2$, since $C_3(\theta) = C_2(-\theta)$ because of the symmetry of the initial configuration.

[31] The consequences of the first hypothesis have been studied in [32] where, for example, the probability distribution of the $\dot{s}_j^-$ was calculated. We will see in the next sections that the second hypothesis does not hold for loops. It will turn out that most kinks on loops have a small amplitude. The flat distributions we use here should be interpreted as a working hypothesis adopted for now in the absence of a concrete dynamical model.

[32] E. J. Copeland, T. W. B. Kibble, and D. A. Steer, Phys. Rev. D **75**, 065024 (2007).

[33] Numerically we have found no example of a simultaneous triple amplification (no matter how large the number of random configurations generated). We have checked that $P(C_1 \geq \alpha, C_2 \geq \alpha, C_3 \geq \alpha)$ is nonzero for any value of $\alpha$ strictly smaller than 1 (increasing the number of configurations always ends up yielding such an event) but this vanishes to zero when $\alpha = 1$.

[34] In fact this is not exactly true if the constant invariant lengths of the strings are exactly equal. In this case, e.g., with $K = 1$, the second generation kinks reach the second junction simultaneously and therefore recombine into a single kink per string instead of three. From then onwards, the total number of kinks in the system would remain constant and equal to three. We disregard this possibility and assume that, because of variations in the length of the strings when their evolutions are taken in account, the three kinks arrive at different times at the junctions giving rise to nine kinks.

[35] This is because as long as the number of kinks is small, the random values of the $C_j$ that are drawn crucially affect the distribution of kinks.

[36] Empirically we find the slope of $\log Q_j^A(n)$ is independent of $j$ for large $n$.

[37] R. Brandenberger, H. Firouzajhi, J. Karouby, and S. Khosravi, Phys. Rev. D **80**, 083508 (2009).

[38] T. W. B. Kibble and N. Turok, Phys. Lett. **116B**, 141 (1982).

[39] N. Turok, Nucl. Phys. **B242**, 520 (1984).

[40] A. L. Chen, D. A. DiCarlo, and S. A. Hotes, Phys. Rev. D **37**, 863 (1988).

[41] D. DeLaney, K. Engle, and X. Scheick, Phys. Rev. D **41**, 1775 (1990).

[42] X. A. Siemens and T. W. B. Kibble, Nucl. Phys. **B438**, 307 (1995).

[43] Note that since we work in flat space, our discussion only applies to subhorizon loops. Indeed, for large loops in an expanding universe, the equations of motion are different from those of Sec. II [44], and for example, the amplitude of a kink decreases while it propagates on a piece of string

from one junction to another [45]. (However, we expect the transmission coefficients computed in Sec. III to remain essentially unchanged since transmissions are instantaneous processes.)

[44] H. Firouzjahi, S. Khoeini-Moghaddam, and S. Khosravi, Phys. Rev. D **81**, 123506 (2010).

[45] E. J. Copeland and T. W. B. Kibble, Phys. Rev. D **80**, 123523 (2009).

[46] The amplitude of the kink transmitted to the light string depends crucially on the configuration, as indicated by the relatively flat distribution of $C_2$.

[47] C. Bachas, Ann. Phys. (N.Y.) **305**, 286 (2003).